FLIGHT MECHANICS AND MONTE CARLO ANALYSIS FOR A STUDENT SOUNDING ROCKET

Eduardo Jourdan, eduardojourdan92@gmail.com[1]
Dalton Menezes, daltonmenezes93@gmail.com[1]
Matheus Ferraz, matheusc.ferraz18@gmail.com[1]
Luis Fernando Gonçalinho Antonio, lfergon191@gmail.com[1]

[1]*Instituto Tecnológico de Aeronáutica, 12228-900 São José dos Campos, SP, Brazil*

Abstract: *During these past five years a student group in Instituto Tecnológico de Aeronáutica (ITA) called ITA Rocket Design has been developing and flying high-power rockets in order to participate in an international college engineering competition called IREC that is held every year in the United States. The objective of this competition is to build, test and fly experimental sounding rockets to achieve as close as possible 10000 ft carrying 10 lb of payload and recover it. Their flight envelope involves a very high acceleration from launch, no guidance and control during ascent and a smooth descent and recovery via parachutes. This present work describes the analysis of flight mechanics performed in order to do system design and to derive subsystem requirements. A computational framework was made in Matlab and C++ language to perform point-mass simulations to determine propellant and structural mass and a high fidelity 6 DOF simulator for Monte Carlo simulations. Different analysis are performed such as a comparison between different aerodynamic models in the 6DOF simulator and a study on the wind model influence on stability parameters. Finally, Monte Carlo simulations are considered in order to study the sensitivity of the apogee altitude, maximum velocity, maximum acceleration and launch rail exit velocity regarding parameters uncertainties, including aerodynamic model and thrust model errors. The results indicate that wind velocity is an important aspect regarding horizontal velocity at apogee and thus it is a major issue when designing the recovery subsystem. Moreover, aerodynamic damping coefficients have a huge impact in the flight dynamics but not as much in performance parameters such as apogee altitude and maximum velocity.*
Keywords: *Flight Mechanics, Monte Carlo, Flight Stability, High fidelity simulation*

1. INTRODUCTION

During these past five years a student group in Instituto Tecnológico de Aeronáutica (ITA) called ITA Rocket Design has been developing and flying high-power rockets. The main objectives of this group are to encourage engineering students to pursuit a degree in aerospace and to give hands-on experience in design, testing and flying rockets. Major subjects of those projects are flight mechanics and stability, both necessary to evaluate the rocket performance and launch safety. This paper main objective is to describe the several analysis performed during all project phases with different flight simulation models and discuss their results.

Since 2011, ITA Rocket Design has been participating in the Intercollegiate Rocket Engineering Competition (IREC), the world's largest university rocket engineering competition (Mueller, 2016). IREC is organized every year by an American organization called Experimental Sounding Rocket Association (ESRA). ESRA is a non-profit organization founded in 2003 for the purpose of fostering and promoting engineering knowledge and experience in the field of rocketry. This competition is held every year in June in a city called Green River located in Utah, US. Its challenge is to design, build, test and fly experimental sounding rockets to achieve as close as possible 3km carrying a 4.5kg payload and recovery it. Therefore, the goal is not to reach as high as possible, but accurately 3 km.

So altogether, the project of a rocket able to compete in IREC has two main requirements regarding flight mechanics: the rocket shall achieve an apogee inside 3 ± 0.1 km carrying a minimal weight of 4.5 kg of payload and the rocket shall have a stable flight during ascent phase (Mueller, 2016). The first objective of the flight mechanics design team is, from those two statements, derive requirements for the propulsion and structural subsystems. The requirements here considered are the total impulse of the motor and the structural mass interval that together makes possible to achieve the apogee of 3 ± 0.1 km. At this point, the project is still in its conceptual and preliminary phase and so the amount of information available of the rocket is limited. Therefore, this first analysis is performed considering two degree of freedom (DOF) flight simulation in Matlab environment. In this simulation the rocket is simple considered a point-mass with a reference area used for drag calculation.

In the scope of the ITA Rocket Design team, the other goal of stable flight ascent is also considered during preliminary design by the flight mechanics subsystem. The sounding rocket typically has fins for that very objective, that is to bring the center of pressure (C_p) backward in relation to the center of mass (CG) (Nakka, 2015). The IREC has a rule imposing that the margin static shall be in the interval of one to two calibers during all ascent flight, where margin static is the distance from CG and C_p and caliber is a distance unit divided by the rocket larger diameter. The ITA Rocket Design team developed a computational framework with C++ language, Matlab and Missile Datcom Softwares in order to perform flight stability analysis and to size the fins during the preliminary project. This tool is described in this paper.

As the rocket design goals from system to subsystem and components, more information is available for improving the simulations. The final objective of flight mechanics subsystem is to verify by means of flight simulations if the mission

goals for the IREC are all achieved by the final rocket design. In this analysis, a high fidelity six DOF C++ flight simulator developed by ITA Rocket Design is used to perform Monte Carlo simulations. Those simulations are described in this work and they include a more accurate aerodynamic model, several model perturbations and a more realistic environment. With that in mind, this paper is organized as follows: Section 2describes the flight simulation models used in the 2DOF and 6DOF simulators as well as the equations of motion considered in both of them; Sec. 3shows the results for each one of the simulations cited above and Sec. 4describes the main concluding remarks.

2. FLIGHT SIMULATION MODELS

This section describes the models and equations of motion considered in the 2DOF and 6DOF flight simulations. The 2DOF simulator is implemented in a Matlab environment where it is easier to change inputs. One of the 6DOF objectives is to perform Monte Carlo simulations, where the code performance and run time aspects are much more important. Due to this, it is implemented using C++ language and has parallel computation capability by means of shared-memory programming with OpenMP. The input and output is performed with text files, and Matlab scripts are used to facilitate the final user work of running jobs and analyze results.

2.1 2 DOF Longitudinal Flight simulation

This simulation is intended for preliminary design, where rapid simulations are needed and a lot of different designs are tested. The main performance parameters to evaluate with this simulator are the apogee altitude, maximum velocity, maximum acceleration and the exit velocity from the launch rail. The rocket is considered a simple point-mass with total mass M and reference area S. The flight is in a vertical plane and the rocket has no lateral motion and do not spin. Thus, the movement can totally be described by an horizontal linear speed V_x and a vertical linear speed V_y. The system origin is the launch site, the X axis is tangential to the ground and the Y axis is pointing upwards.

In this simulation the equations of motion are as follows

$$\gamma = \arctan(V_y/V_x)\,, \tag{1}$$

$$M_p = M_{\text{p,initial}} \cdot (1 - t/t_b)\,, \tag{2}$$

$$\begin{aligned} D_x &= 0.5 \cdot \rho \cdot S \cdot C_D \cdot V_x^2\,, \\ D_y &= 0.5 \cdot \rho \cdot S \cdot C_D \cdot V_y^2\,, \end{aligned} \tag{3}$$

$$\begin{aligned} \dot{V_x} &= (T_{\text{thrust}} \cos(\gamma) - sign(V_x) D_x)/M\,, \\ \dot{V_y} &= (T_{\text{thrust}} \sin(\gamma) - sign(V_y) D_y)/M - g\,, \end{aligned} \tag{4}$$

where γ is the flight path angle. The only aerodynamic force considered is the drag force. It is applied parallel to the velocity vector and the drag coefficient C_D is considered constant for all flight. Since the rocket is a point-mass, the angle of attack is considered zero during all time. The propulsion is modeled by a constant force T_{thrust} and a burning time of t_b. The propellant mass M_p is obtained from linear interpolation until is reaches zero at instant t_b. The total mass M is the sum of structural mass M_{empty} and M_p. The thrust is imposed also parallel to the vector velocity and therefore the only force that changes the flight path angle is gravity since it always points downwards. The gravitational acceleration g is considered constant and equals to 9.801 m/s^2. The air density ρ used for the dynamics pressure calculation is taken from the International Standard Atmosphere (ISA) model. The launch altitude from Green River, Utah is 1300 meters and the apogee is around 3 km, so the influence of altitude in the density becomes important.

During the phase where the rocket is still coupled in the launch rail, the equation 4 change. A fictitious force is summed in order to maintain the flight path angle equal to the launch elevation angle. The time marching scheme considered for this simulator is a four stage fourth order Runge Kutta method. The time step is constant and equals to 0.01 s. The run time for a typical simulation with 25 seconds of flight is around 0.17 s.

2.2 6 DOF Flight simulation

2.2.1 Equations of Motion

This simulator is intended to have much higher fidelity models than the one described in Sec. 2.1The rocket is allowed to move in all three directions and to rotates in all three axes. When perturbations are summed, such as wind, the flight is not carried in a vertical plane anymore. The flat-Earth reference system is considered, where the origin is placed in the launch site with both X and Y axes in the local horizontal plane. The X axis have the same direction as the launch rail with the Y axis making 90° degrees clockwise and the Z axis pointing downwards. For the purpose of this work this is considered an inertial system since the flight time is short and apogee is small compared to the Earth‘s rotation period and Earth‘s radius respectively (Stevens and Lewis, 2003).

Another relevant reference system used is the body system, which is not an inertial system. It is placed in the center of mass of the rocket, moving and rotating attached to the vehicle. The conventional 3-2-1 sequence is considered for the Euler angles (ψ, θ, ϕ) determination, but actually the quaternions (q_0, q_1, q_2, q_3) are used in the kinematics equations to

avoid the singularity at $\theta = 0°$ that is very close to the launch condition. The transformation matrix T_{bi} from the inertial system to the body system and the expressions relating Euler angles and quaternions are

$$\begin{bmatrix} \psi \\ \theta \\ \phi \end{bmatrix} = \begin{bmatrix} arctan(\frac{2(q_1q_2+q_0q_3)}{q_0^2+q_1^2-q_2^2-q_3^2}) \\ arcsin(-2(q_1q_3+q_0q_2)) \\ arctan(\frac{2(q_2q_3+q_0q_1)}{q_0^2-q_1^2-q_2^2+q_3^2}) \end{bmatrix}, \tag{5}$$

$$\boldsymbol{T_{bi}} = \begin{bmatrix} q_0^2+q_1^2-q_2^2-q_3^2 & 2(q_1q_2+q_0q_3) & 2(q_1q_3-q_0q_2) \\ 2(q_1q_2-q_0q_3) & q_0^2-q_1^2+q_2^2-q_3^2 & 2(q_2q_3+q_0q_1) \\ 2(q_1q_3+q_0q_2) & 2(q_2q_3-q_0q_1) & q_0^2-q_1^2-q_2^2+q_3^2 \end{bmatrix}. \tag{6}$$

The vehicle linear velocity is described in the body system by the vector (u, v, w). Moreover, the angular velocity of the body frame relative to the inertial system has the components (p, q, r) described in the body reference system. The following expressions are the kinematics equations of motion, in which linear and angular velocities are related to translational position (x, y, z) and quaternions,

$$\begin{bmatrix} \dot{x} \\ \dot{y} \\ \dot{z} \end{bmatrix} = \boldsymbol{T_{bi}^{-1}} \begin{bmatrix} u \\ v \\ w \end{bmatrix}, \tag{7}$$

$$\begin{bmatrix} \dot{q_0} \\ \dot{q_1} \\ \dot{q_2} \\ \dot{q_3} \end{bmatrix} = \begin{bmatrix} 0.5(-p \cdot q_1 - q \cdot q_2 - r \cdot q_3) \\ 0.5(p \cdot q_0 + r \cdot q_2 - q \cdot q_3) \\ 0.5(q \cdot q_0 - r \cdot q_1 + p \cdot q_3) \\ 0.5(r \cdot q_0 + q \cdot q_1 - p \cdot q_2) \end{bmatrix}. \tag{8}$$

Besides the seven kinematics equations of motion shown in 7 and 8, there are more six others differential equations to be resolved that describes the dynamics of the system. They relate linear and angular acceleration to linear and angular velocities:

$$\begin{bmatrix} \dot{u} \\ \dot{v} \\ \dot{w} \end{bmatrix} = \begin{bmatrix} r \cdot v - q \cdot w + (F_{\text{aero}_x} + T_{\text{thrust}})/M + \boldsymbol{T_{bi}}(1,3)g \\ w \cdot p - r \cdot u + (F_{\text{aero}_y})/M + \boldsymbol{T_{bi}}(2,3)g \\ q \cdot u - p \cdot v + (F_{\text{aero}_z})/M + \boldsymbol{T_{bi}}(3,3)g \end{bmatrix}, \tag{9}$$

$$\begin{bmatrix} \dot{p} \\ \dot{q} \\ \dot{r} \end{bmatrix} = \begin{bmatrix} ((I_y - I_z)qr + M_{\text{aero}_x})/I_x \\ ((I_z - I_x)pr + M_{\text{aero}_y})/I_y \\ ((I_x - I_y)pq + M_{\text{aero}_z})/I_z \end{bmatrix}. \tag{10}$$

The body axis are considered to be the principal axis of the vehicle as the rocket consists of a perfect symmetric body. The variables (I_x, I_y, I_z) are the principal moments of inertia and M is the vehicle's mass, all fully described in Sec. 2.2 .3 The variables $(F_{\text{aero}_x}, F_{\text{aero}_y}, F_{\text{aero}_z}, M_{\text{aero}_x}, M_{\text{aero}_y}, M_{\text{aero}_z})$ are the forces and moments generated by aerodynamics and are fully described in Sec. 2.2.2

Altogether, the rocket is totally described by 13 states $(x, y, z, u, v, w, q_0, q_1, q_2, q_3, p, q, r)$ and 13 differential equations. When the vehicle is in the launch rail, the equations are modified to maintain its pitch angle the same as the launch rail angle. All derivatives $(\dot{v}, \dot{w}, \dot{q_0}, \dot{q_1}, \dot{q_2}, \dot{q_3}, \dot{p}, \dot{q}, \dot{r})$ are zero, equation 7 is used and also $\dot{u} = (F_{\text{aero}_x} + T_{\text{thrust}})/M - sin(\theta)g - \mu cos(\theta)g$, where μ is the dynamic friction coefficient of the rail. A second-order Adam-Bashforth method is used to integrate the equations with 0.001 s of time step. The total run time for 30 seconds of flight is typically 0.2 s. Besides, the simple explicit Euler scheme is used to initialize the equations.

2.2.2 Aerodynamic Model

The aerodynamic model is responsible for calculating the aerodynamic forces and moments defined by the variables $(F_{\text{aero}_x}, F_{\text{aero}_y}, F_{\text{aero}_z}, M_{\text{aero}_x}, M_{\text{aero}_y}, M_{\text{aero}_z})$. The inputs for this model are: altitude (h), linear velocities (u, v, w), angular velocities (p, q, r), linear velocities derivatives $(\dot{u}, \dot{v}, \dot{w})$, position of the center of mass (CG) and wind velocity in the body axes $(u_{wind}, v_{wind}, w_{wind})$. There are four constant parameters that are necessary: longitudinal reference (c), lateral reference (lat_{ref}), area reference (S_{ref}) and the position of the moment center of reference (CRM).

First, the wind influence is determined by defining the relative velocity of the vehicle to the air in the body system as $(u_{air}, v_{air}, w_{air}) = (u, v, w) - (u_{wind}, v_{wind}, w_{wind})$, with magnitude V. At each instant the angle of attack (α), slip angle (β) and also $\dot{\alpha}$ are calculated by

$$\alpha = \arctan(\frac{w_{air}}{u_{air}}), \tag{11}$$

$$\beta = \arcsin(\frac{v_{air}}{V}), \tag{12}$$

$$\dot{\alpha} = \frac{u_{air} \cdot \dot{w} - w_{air} \cdot \dot{u}}{u_{air}^2 + w_{air}^2}, \tag{13}$$

The density ρ and temperature T are obtained as a function of altitude from the ISA model, and thus the Mach number is calculated as $\frac{V}{V_{sound}}$.

The forces and moments are calculated by means of 17 coefficients (Blakelock, 1991), all determined with the software Missile Datcom. This software utilizes semi-empiric methods, empirical corrections and interference coefficients between body and fins to determine them. The coefficients considered are:

$$\begin{aligned}
CA &= \text{axial force coefficient ,} \\
CA_q &= \text{axial force coefficient derivative with pitch rate ,} \\
CY &= \text{side force coefficient ,} \\
CY_p &= \text{side force coefficient derivative with roll rate ,} \\
CY_r &= \text{side force coefficient derivative with yaw rate ,} \\
CN &= \text{normal force coefficient ,} \\
CN_q &= \text{normal force coefficient derivative with pitch rate ,} \\
CN_{\dot{\alpha}} &= \text{normal force coefficient derivative with rate of change of angle of attack ,} \\
CLL &= \text{rolling moment coefficient ,} \\
CLL_r &= \text{rolling moment coefficient derivative with yaw rate ,} \\
CLL_p &= \text{rolling moment coefficient derivative with roll rate ,} \\
CLM &= \text{pitching moment coefficient ,} \\
CLM_q &= \text{pitching moment coefficient derivative with pitch rate ,} \\
CLM_{\dot{\alpha}} &= \text{pitching moment coefficient derivative with rate of change of angle of attack ,} \\
CLN &= \text{yawing moment coefficient ,} \\
CLN_r &= \text{yawing moment coefficient derivative with yaw rate ,} \\
CLN_p &= \text{yawing moment coefficient derivative with roll rate .}
\end{aligned} \tag{14}$$

A computational tool was developed in C++ in order to obtain these coefficients in all flight envelope: $-20^\circ < \alpha < 20^\circ$, $-20^\circ < \beta < 20^\circ$ and $0 < Mach < 0.8$. This tool is called prior to the very flight simulator in order to create one look-up table for each one of the 17 coefficients. These tables are loaded in the beginning of the simulation and have three indexes: angle of attack, slip angle and Mach number. The interval of α is divided in 20 equally spaced points, β in 30 equally spaced points and Mach number in 8 points (0.05, 0.1, 0.2, 0.3, 0.4, 0.5, 0.6, 0.8). At each instant, each coefficient is obtained from its table by means of multi-linear interpolation between the nearest points of the table. The coefficients are considered constant outside of the their intervals of variation.

After the coefficients are determined from the look-up tables, then the forces and moments are calculated by

$$\begin{aligned}
C_X &= -(CA + CA_q * lat_{ref} * q/V) , \\
C_Y &= CY + CY_p * lat_{ref} * p/V + CY_r * lat_{ref} * r/V , \\
C_Z &= -(CN + CN_q * c * q/V + CN_{\dot{\alpha}} * c * \dot{\alpha}/V) , \\
CLL &= CLL + CLL_r * lat_{ref} * r/V + CLL_p * lat_{ref} * p/V , \\
CLM &= CLM + CLM_q * c * q/V + CLM_{\dot{\alpha}} * c * \dot{\alpha}/V - C_Z * (CG - CRM)/c , \\
CLN &= CLN + CLN_r * lat_{ref} * r/V + CLN_p * lat_{ref} * p/V - C_Y * (CG - CRM)/lat_{ref} .
\end{aligned} \tag{15}$$

It is important to notice the minus signal in some of the definitions above. They are a transformation of the reference system from Missile Datcom and the body system used in the flight simulator. Besides, for the moments its necessary to do a shift since CRM and CG are not necessary at the same position. Finally, the expression of the forces and moments are

$$\begin{aligned}
Faero_x &= 0.5 * \rho * V^2 * S_{ref} * C_X , \\
Faero_y &= 0.5 * \rho * V^2 * S_{ref} * C_Y , \\
Faero_z &= 0.5 * \rho * V^2 * S_{ref} * C_Z , \\
Maero_x &= 0.5 * \rho * V^2 * S_{ref} * lat_{ref} * CLL , \\
Maero_y &= 0.5 * \rho * V^2 * S_{ref} * c * CLM , \\
Maero_z &= 0.5 * \rho * V^2 * S_{ref} * lat_{ref} * CLN .
\end{aligned} \tag{16}$$

As can be seen in Eq. 15, the damping coefficients are taking into account by the aerodynamic model. A flag variable is utilized in order to turn them on/off.

2.2.3 Propulsion, Inertia and Environment Models

The propulsion model can be either experimental results from a static test of the motor or a constant force T_{thrust} acting during t_b seconds. The force is assumed to be in the x body axis. The inertia parameters are the mass M and the

principal moments of inertia (I_x, I_y, I_z). They are calculated by a linear interpolation between their values at $t = 0$ and $t = t_b$. After the motor stops burning, they remain constant. The CG position is assumed to be in the longitudinal axis of the rocket since it is symmetric. Its position is also determined by linear interpolation between its value at $t = 0$ and $t = t_b$.

In this work, the environment parameters are the air properties obtained from ISA model and a constant wind. The wind is assumed to have constant velocity vector of magnitude V_{wind} and it is always parallel to the ground, with heading ψ_{wind} being also a parameter. A value $\psi_{wind} = 0°$ means that the wind have the same direction as the launch rail and $\psi_{wind} = 90°$ means that it points to the right.

3. RESULTS

The numerical results presented here describe the various flight simulations and flight mechanics analysis done during all project phases of the student sounding rocket. Simulations are done with the 2DOF simulator and a 6DOF simulator discussed in Sec. 2.

3.1 Conceptual Phase: Deriving Requirements

This sections describes the flight mechanics simulations performed to derive the main mission requirements into propulsion and structures requirements. The main requirement is: the rocket shall achieve an apogee inside 3 ± 0.1 km carrying a minimal weight of 4.5 kg of payload. With that in mind, the objective of this analysis is to determine an interval of structural mass and total motor impulse that achieves the mission. The 2DOF flight simulator is used since there is little information about the rocket geometry and properties as this is still the conceptual and preliminary phase.

For the simulation to be carried out, a baseline rocket is chosen based on the previous group experience with the characteristics presented in Table 1. As described in Sec. 2.1 the drag coefficient is constant during all flight and the propulsion thrust is made constant during 4 seconds. For each total impulse considered, the propellant mass is calculated based on a baseline specific impulse (Isp) of 112 seconds. This Isp value was achieved in previous rocket solid motors developed by ITA Rocket Design. The altitude in Table 1 is the altitude of the city of Green River, UT, where the competition IREC occurs. The rail characteristics are provided by the IREC organizers.

Tabela 1: Baseline rocket characteristics for deriving requirements.

CD	0.3
Altitude	1305.1 m
Burning time	4 s
Impulse specific	112 s
Launch angle	83° s

Various simulations are performed with different motor total impulse and rocket empty mass and the results are shown in Fig. 1. In Fig. 1(a), it is possible to notice a green interval in which the apogee is 3km as requested by IREC. That same area in figures 1(b) and 1(c) indicates a maximum flight Mach number around 0.7 and 22 m/s of velocity at launch rail exit. Other simulations are done considering a baseline empty mass of 22 kg and a total impulse of 7850 Ns to evaluate flight characteristics sensitivity to some parameters, such as CD, burning time and launch angle. Each parameter is changed separately, keeping the others constant and equals to the baseline values.

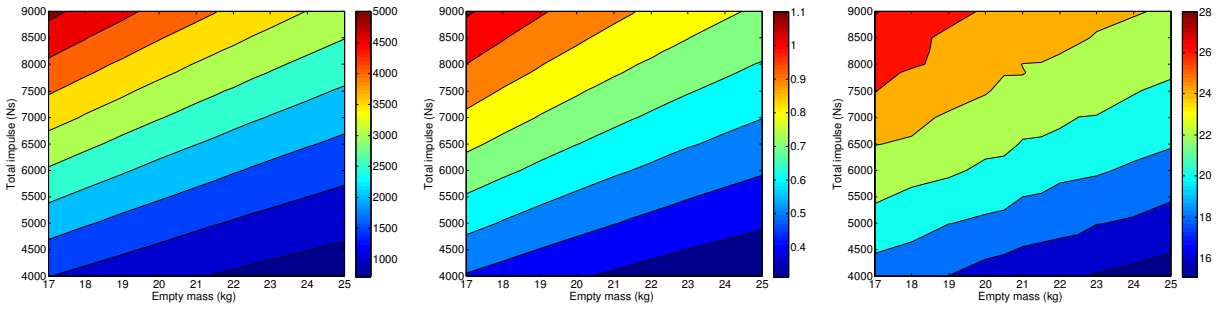

(a) Flight apogee (m). (b) Flight maximum Mach number. (c) Ramp exit velocity (m/s).

Figura 1: Flight apogee, maximum velocity and ramp exit velocity as a function of total impulse and empty mass.

It can be seen in Fig. 2 that, in the ITA Rocket Design context, CD has a significant impact in the flight apogee but do not have much influence in maximum velocity and ramp exit velocity. Increasing the CD value from 0.3 to 0.4 diminish the apogee from 3200 to 3000 meters. On the other hand, Fig. 3 shows that the burning time affects all three main flight characteristics but it is mainly an important design parameter for stability right after launch since it changes dramatically the ramp exit velocity. Lastly, Fig. 4 indicates that the launch angle does not affect maximum velocity and ramp exit

velocity and that it can be used as a parameter to change at least 250 meters of apogee. The IREC only allows launch from 80 to 86 degrees of elevation.

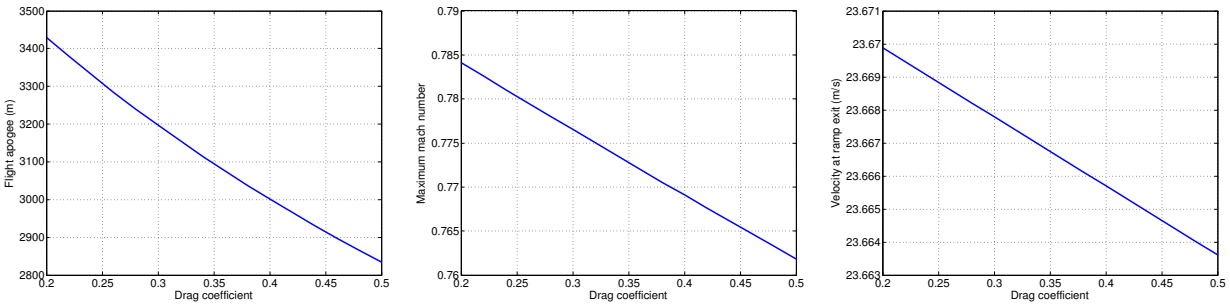

(a) Flight apogee (m). (b) Flight maximum Mach number. (c) Ramp exit velocity (m/s).

Figura 2: Flight apogee, maximum velocity and ramp exit velocity as a function of drag coefficient.

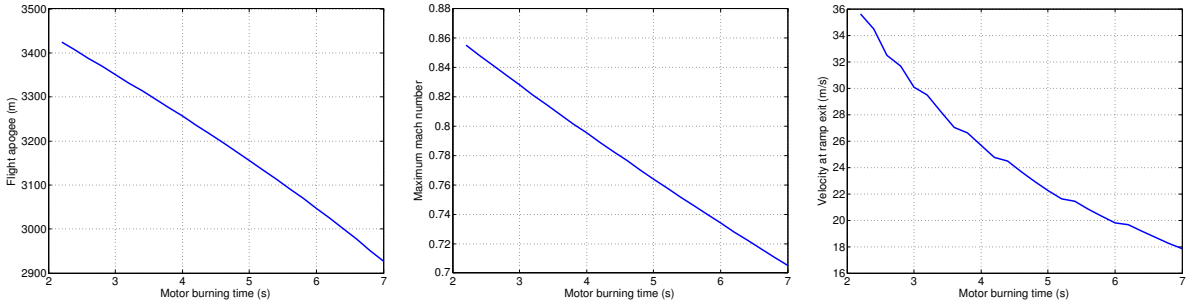

(a) Flight apogee (m). (b) Flight maximum Mach number. (c) Ramp exit velocity (m/s).

Figura 3: Flight apogee, maximum velocity and ramp exit velocity as a function of motor burning time.

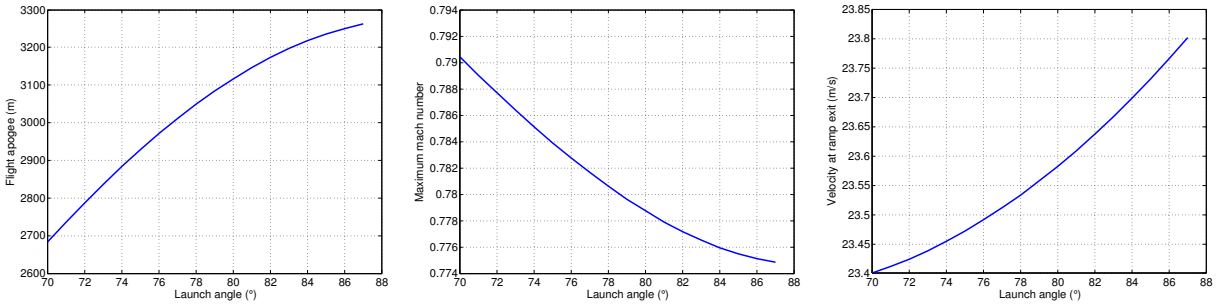

(a) Flight apogee (m). (b) Flight maximum Mach number. (c) Ramp exit velocity (m/s).

Figura 4: Flight apogee, maximum velocity and ramp exit velocity as a function of launch angle elevation.

3.2 Preliminary Design: Fin Sizing

Another major task for the flight mechanics and aerodynamics team is to design the fins of the rocket. To the vehicle be stable the CP must be located closer to the nozzle end than the CG, and therefore fins are necessary. Without fins, the CP should be located around the nosecone, above the rocket's CG. IREC's rules dictate that the static margin, the distance between CP and CG, shall be between one and two calibers during the flight, where caliber is the larger diameter of the rocket.

For the CP calculation, the most important parameter is the total wet area of all fins. The fin format and configuration influences more how the CP varies with angle of attack and Mach number, but its location at zero angle of attack is mainly dictated by the fin's area. The fin airfoil section geometry is also an important parameter primarily for drag effects, but for ease of construction it is made a simple flat plate with some very small chamfer in the leading and trailing edges.

A computational tool was made in C++ language in order to integrate Missile Datcom input/output and to analyze the results. Each run of the Missile Datcom only allows one slip angle of flight condition, despite the fact that it allows 20 values of angle of attack and 10 for Mach number. Therefore, the computational tool runs several times Datcom and it assemblies the aerodynamic model of the rocket as described in Section 2.2.2 This same tool is used to construct the models for the 6DOF flight simulators and it helps the user to set the Datcom inputs since they are not intuitive and require some experience with the program.

In this work, the fin shape is made clipped delta, with a root chord of 2D, tip chord of 1D and 1D of span, where D is a design parameter to be determined. The leading edge has 45 degrees of sweep angle and a number of three fins instead of four is chosen in order to reduce drag. This fin plat format is chosen due to the group experience for the ease of manufacturing. The nosecone is made elliptic with a fineness ratio of 2 since the flight does not achieve high supersonic velocities and ITA Rocket Design already has a metal mold of this size to be used in the manufacturing process of the fiberglass nosecone. Finally, from preliminary design in a CAD software, the total rocket length is estimated as 2.38 m. Also, the CG of the rocket including or not the propellant mass can be already estimated as 2.38 m, 1.61 m (with propellant) and 1.5 m (empty) respectively. The CG is measured taking from reference the tip of the nosecone and as the rocket diameter is 5 inches, or 0.127 m, then the CG drift is of 0.86 calibers. It is important to ensure that the rocket is stable during all flight, and therefore in all CG changing interval. One relevant observation is that the rocket diameter is a design parameter derived mainly for propellant volume reasons and recovery operation easiness, as the rocket length is determined after subsystems preliminary design.

The parameter D of the fin is chosen to be 107.5 mm and it can be seen in Fig. 5 the variation of static margin regarding angle of attack and Mach number for two configurations, motor empty and loaded. The static margin is given in calibers and should be between 1 and 2 in both cases. It is difficult to achieve those characteristics since the CG drift is around 0.86 as after burning the motor, the CG moves upwards closer to the nosecone and therefore the static margin increases. Nevertheless, in both figures 5(a) and 5(b) the static margin is considered acceptable.

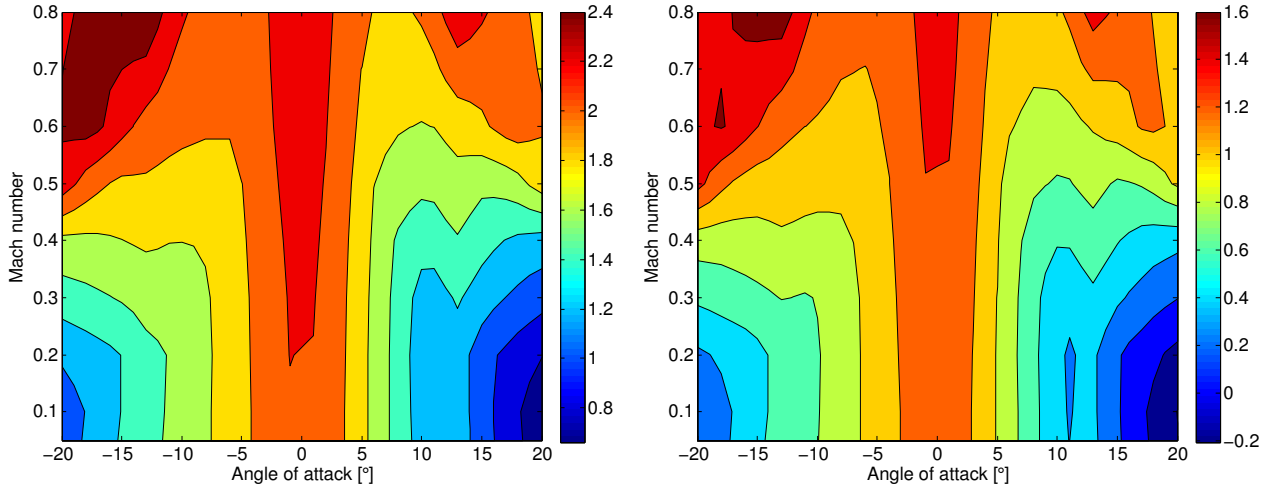

(a) After motor burn.

(b) Before motor burn.

Figura 5: Rocket static margin in calibers as a function of α and Mach number for both empty and loaded motor.

The critical condition is when the rocket leaves the launch rail since its velocity is still low and can be comparable with the wind velocity, resulting in very high angle of attack. As the rocket velocity increases, the wind velocity generates much lower angle of attack. In Fig. 5 it is possible to see that the worst values of static margin are exactly for low velocities and high angle of attack. In order to further analyze this condition, figure 6 shows the static margin for the loaded rocket considering different wind and launch rail exit velocities. For each condition of wind and launch velocity, the mach number and α can be calculated and then the static margin is determined. The wind is considered at 90 degrees with the vehicle in order to generate the larger angle of attack possible and the rocket is considered loaded so as the burning time is much higher than the time to leave the rail. Those are extreme conditions since any propellant that burns helps the CG to move upwards and therefore increases the static margin. Considering a ramp exit velocity of 22 m/s from the fig. 1(c), thus the maximum wind acceptable for launching is 6 m/s.

3.3 Aerodynamic Response to Perturbations

This sections describes analysis of aerodynamic response due to wind perturbations performed with the 6DOF simulator. Various simulations are performed considering different initial conditions and wind levels as well as two different aerodynamics models, one with damping coefficients and another with no damping, both described in Section 2.2.2 The main objectives are to evaluate the influence of the damping coefficients in the aerodynamic response and to visualize the wind affect in the rocket trajectory.

All simulations here are performed with the rocket being initially in horizontal position with 100 m/s of velocity magnitude and no gravity force. Therefore, except for wind perturbations or initial conditions of attack angle and slip angle, the vehicle estimated path shall be an horizontal straight line and its velocity shall decrease with time. The rocket characteristics considered are shown in Table 2. The aerodynamic model is created as described in Sec. 2.2.2with the same geometry as in Sec. 3.2and no motor burning is considered.

First, two simulations are performed with no wind and initial conditions of zero slip angle and 8 degrees of angle of attack. One is performed with damping coefficients included and the other with no damping. The results are shown in Fig.

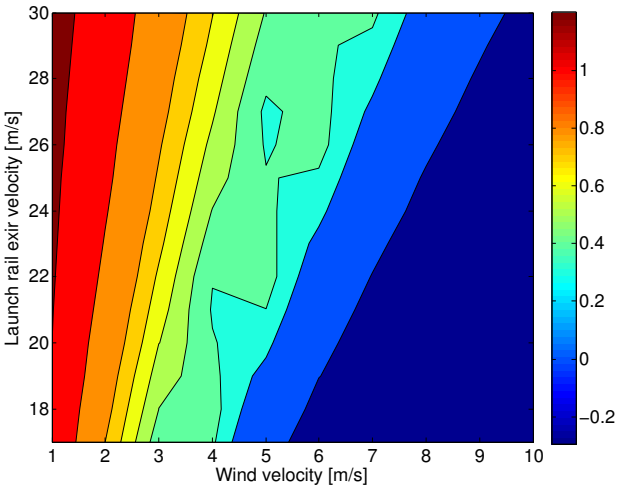

Figura 6: Rocket static margin in calibers as a function of wind and launch rail exit velocities.

Tabela 2: Baseline rocket characteristics of the 6DOF simulations for aerodynamic response analysis.

Altitude	1305.1 m
Total mass	21.9 kg
Ixx	0.066 $kg \cdot m^2$
Iyy	10.743 $kg \cdot m^2$
Izz	10.743 $kg \cdot m^2$
CG	1.5 m from the nosecone tip
Flight time	20 s

7 and it is possible to see that the aerodynamic damping have huge impact. The settling time for the case with damping is around 7 seconds and it is larger than 20 seconds when there is no damping. On the other hand, the frequency natural response almost does not change.

Thus, two simulations are performed with no wind and initial conditions of 8 degrees of slip angle and 8 degrees of angle of attack. Again, one is performed with damping coefficients included and the other with no damping. The results are shown in Fig. 8 and it is possible to see that the aerodynamic damping again have huge impact. Actually, with no damping the roll rate does not goes to zero and α and β don't settle. The response is similar in the case with zero initial conditions of slip angle and angle of attack, but with constant wind velocity of 10 m/s and $\psi = 90°$ of heading, as can be seen in Fig. 9. The aerodynamic damping coefficients are important when aerodynamic coupling and induced roll moments due to different values of α and β impacts are considered in the aerodynamic model.

Lastly, two flight simulations are performed with parameters as in Table 3, with and without damping coefficients. The results are shows in Fig. 10. Again, when there is no damping coefficients, the wind perturbation results in a rolling vehicle and α and β take as least twice the time to settle to zero after the rocket leaves the launch rail. On the other hand, the apogee values don't change significantly between both simulations, only around 10 meters.

Tabela 3: Baseline rocket characteristics of the 6DOF simulations for aerodynamic response analysis.

Altitude	1305.1 m	Flight time	30 s
Mass($t = 0$)	29 kg	Mass($t = t_b$)	21.9 kg
Ixx($t = 0$)	0.079 $kg \cdot m^2$	Ixx($t = t_b$)	0.066 $kg \cdot m^2$
Iyy($t = 0$)	10.743 $kg \cdot m^2$	Iyy($t = t_b$)	8.93 $kg \cdot m^2$
Izz($t = 0$)	10.743 $kg \cdot m^2$	Izz($t = t_b$)	8.93 $kg \cdot m^2$
CG($t = 0$)	1.61 m from the nosecone tip	CG($t = t_b$)	1.5 m from the nosecone tip
Launch rail length	5.48 m	Launch elevation angle	83°
Burn time (t_b)	4.6 s	Thrust	1706 N
Wind velocity	5 m/s	Wind heading (ψ_{wind})	90°
Rail dynamic friction coefficient	0.5		

3.4 Monte Carlo Analysis

A series of Monte Carlo simulations are performed in order to assess the influence of several models used in the 6DOF. First, the wind influence is analyzed. All parameters are constant as displayed in Table 3, except for the wind model. A number of 10000 simulations are performed and in each one the wind velocity and heading is selected randomly from the

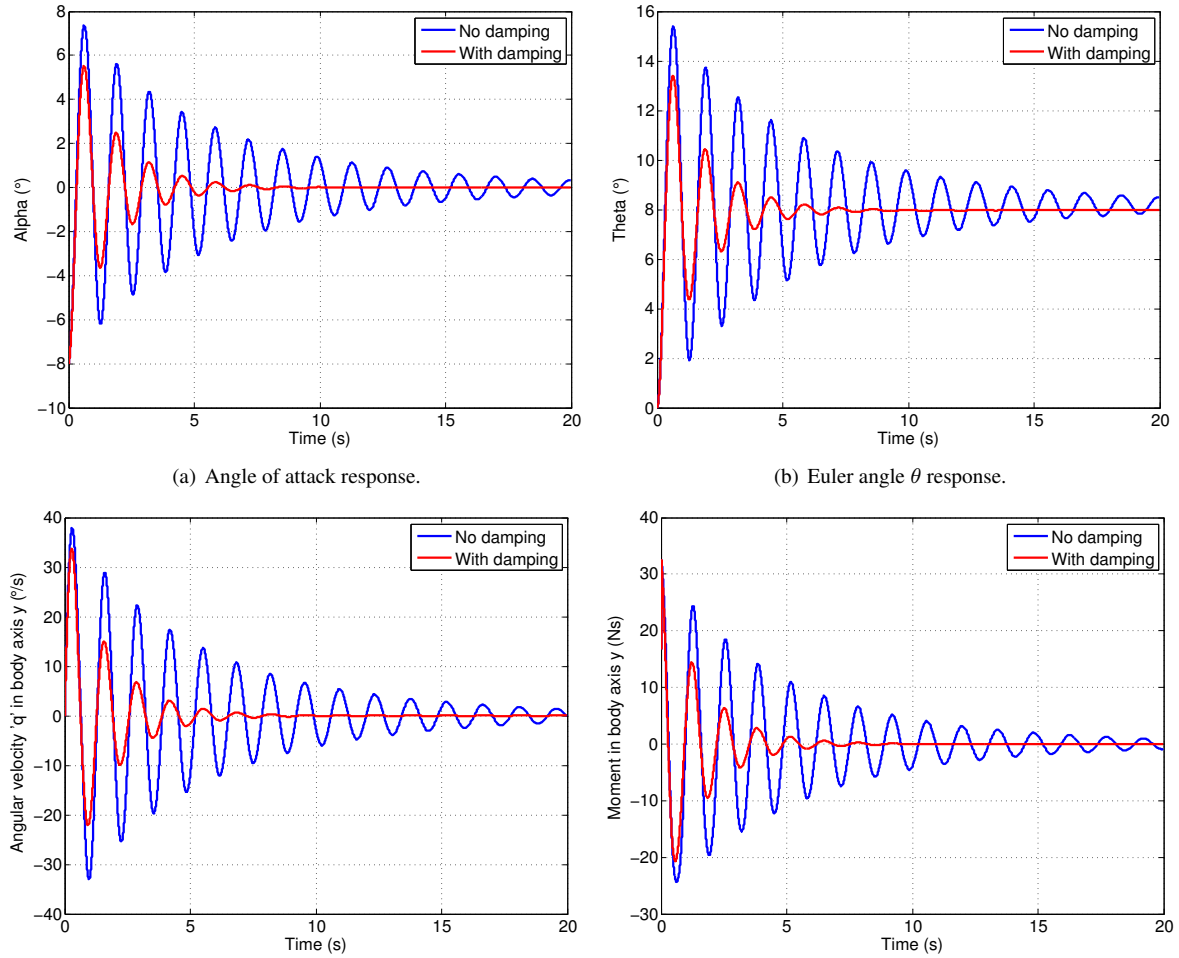

(a) Angle of attack response.

(b) Euler angle θ response.

(c) Angular velocity q response.

(d) Aerodynamic moment in body axis y response.

Figura 7: Comparison of aerodynamic models for the case with initial $\alpha = 8°$, $\beta = 0°$ and no wind velocity.

distributions described in Table 4. The distribution results for some flight mechanics parameters are shown in Fig. 11. The most important aspects influenced by the wind are the apogee with 33 meters of standard deviation and the velocity at apogee with a large six σ interval from 12 m/s to 63 m/s. The velocity at apogee is important for the recovery subsystem design, since it affects the shock absorbed by the chock cords and shear pins.

Tabela 4: Parameters distribution for the wind influence analysis with Monte Carlo simulations.

Wind velocity	Mean	Standard deviation
Gaussian distribution	0	2.3 m/s
Wind heading	Minimum	Maximum
Uniform distribution	0 degrees	360 degrees

Next, the aerodynamic model uncertainties influence is analyzed. A number of 10000 simulations are performed. All parameters are constant as displayed in Table 3, except that there is no wind and some errors are accounted in the aerodynamic model. A proportional error is considered in each one of the six coefficients in Eq. 15. All coefficients have a different error from each other and from each simulation. The final equation used is $\text{Coef} = \text{Coef} \cdot (1 + \text{Coef}_{\text{error}})$, where $\text{Coef}_{\text{error}}$ is randomly selected from a uniform distribution between -0.3 and +0.3. The results for some flight mechanics parameters are shown in Fig. 12. It is interesting to notice that the aerodynamic uncertainties influences more the apogee than the wind model, a result probably due to the drag influence. On the other hand, the wind affect much more the apogee velocity than the aerodynamic model error. Besides, the results of distribution are uniform, as the error model implemented. The aerodynamic errors have minor influence in the other aspects.

The same kind of analysis is considered with the propulsion model and again 10000 simulations are performed. All parameters are constant as displayed in Table 3, except that there isn't wind. The thrust model is still a constant force, but its value is uniformly randomly selected from the interval 1400 to 2000 N. Moreover, the total impulse is randomly selected from a Gaussian distribution of mean 7848 Ns and standard deviation of 400 Ns, 5% of the mean value. The burning time is calculated from the selected force and total impulse. The results for some flight mechanics parameters are shown in Fig. 13. The propulsion model influences hugely all parameters. It can be seen from Fig. 13(a) that the 6σ interval for the apogee is from 2.5 km to 4.5 km, a 2 km difference for only 5% value of standard deviation in the total

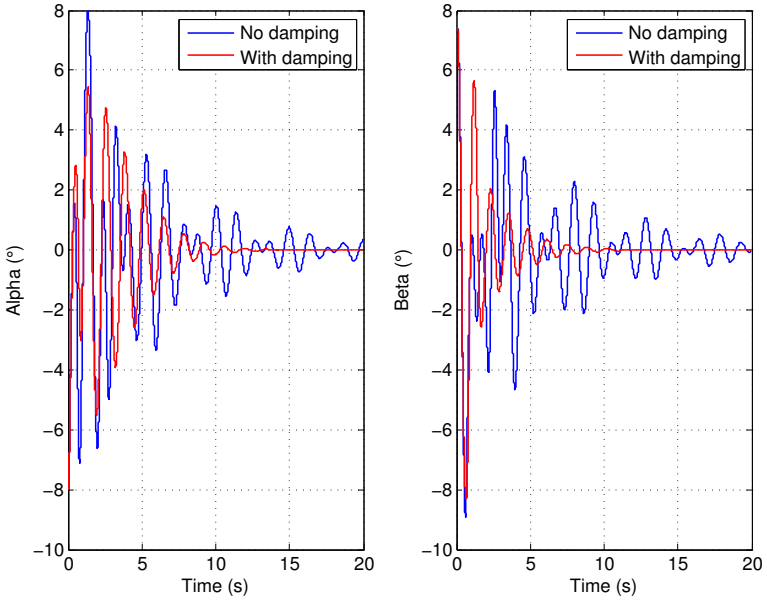

(a) Angle of attack and slip angle response.

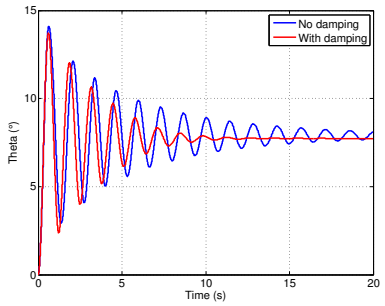

(b) θ response.

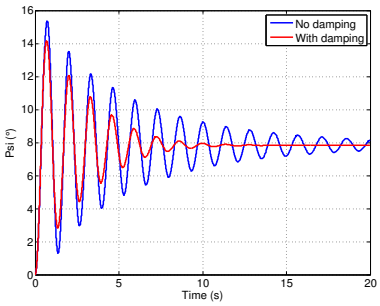

(c) ψ response.

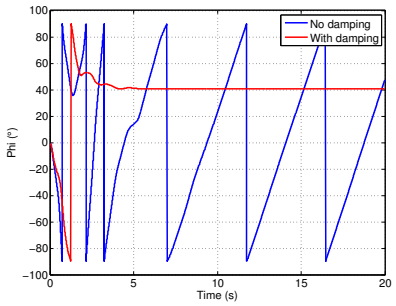

(d) ϕ response.

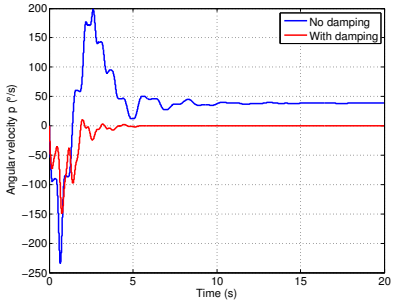

(e) Angular velocity p response.

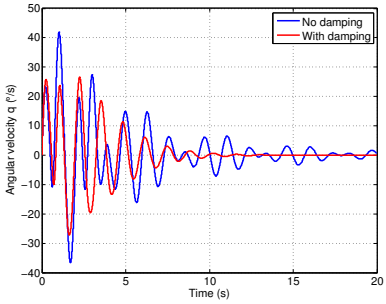

(f) Angular velocity q response.

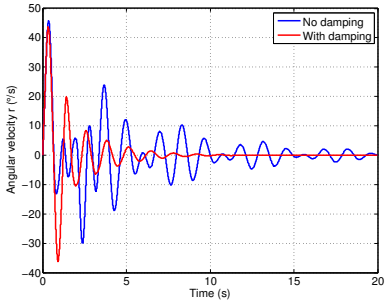

(g) Angular velocity r response.

Figura 8: Comparison of aerodynamic models for the case with initial $\alpha = 8°$, $\beta = 8°$ and no wind velocity.

impulse. Besides, it is interesting to notice that the distribution for apogee, maximum velocity and velocity at apogee are approximately Gaussian distribution, where as the results for maximum acceleration and launch rail exit velocity are a uniform distribution. Thus, the last two parameters probably are more influenced by the thrust force, meanwhile the first three are mainly affected by the total impulse.

Later, a Monte Carlo simulation is performed with all the parameters from aerodynamics, propulsion, wind and inertia models varying together in order to see the final distribution of the flight mechanics performance parameters. The distribution used for each input parameter presented in Table 5 are based on the group's experience and are expectations of the rocket final characteristics after manufacturing. The results from 20000 simulations are shown in Fig. 14. As comparing the figures 13 and 14, it is possible to see that the standard variation for the apogee, maximum velocity, maximum acceleration and ramp exit velocity are mainly influenced by the propulsion model. On the other hand, the velocity at apogee is hugely affected by the wind model and has a very spread probability distribution.

4. CONCLUDING REMARKS

This paper describes the flight mechanics simulations and analysis performed in the student sounding rocket project of ITA Rocket Design, a rocketry group from Instituto Tecnológico de Aeronáutica (ITA). This group goal is to participate

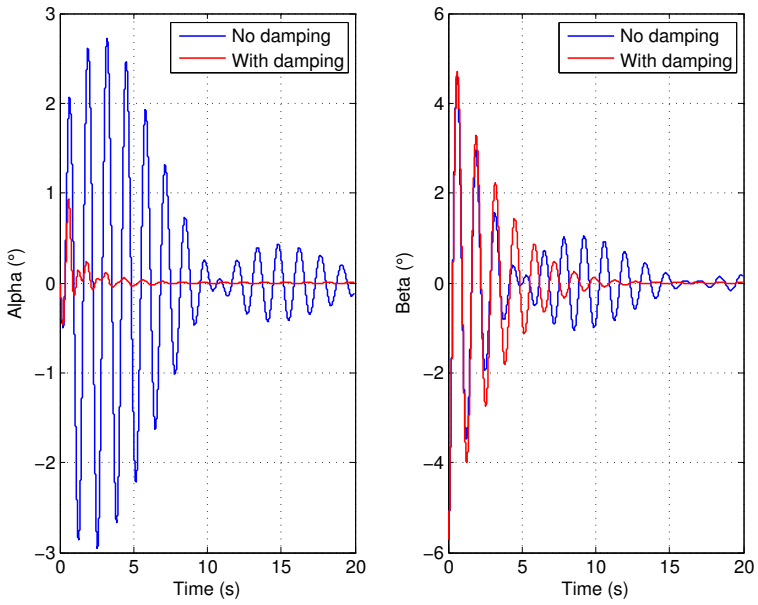

(a) Angle of attack and slip angle response.

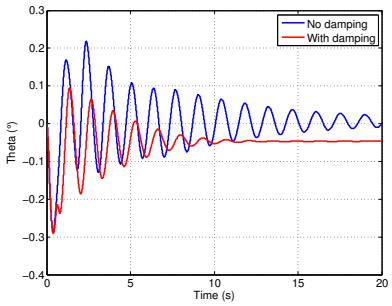

(b) θ response.

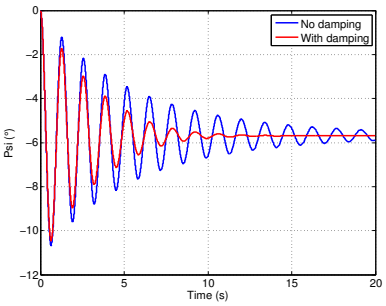

(c) ψ response.

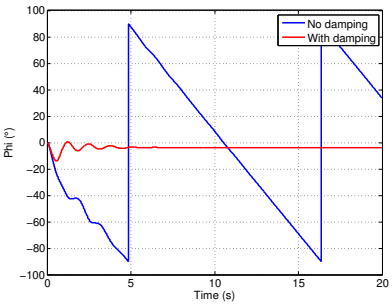

(d) ϕ response.

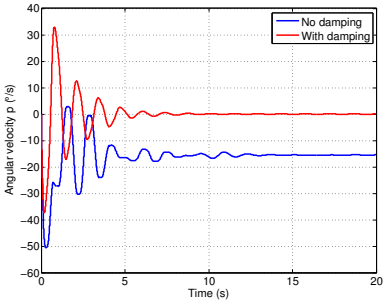

(e) Angular velocity p response.

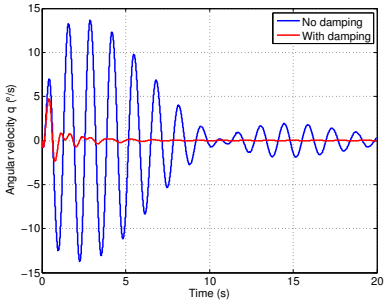

(f) Angular velocity q response.

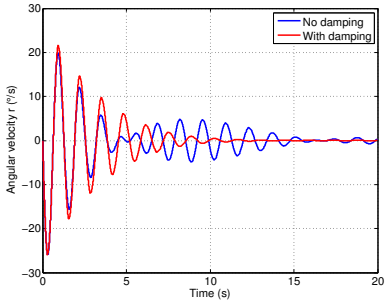

(g) Angular velocity r response.

Figura 9: Comparison of aerodynamic models for the case with initial $\alpha = 0°$, $\beta = 0°$, wind velocity of 10 m/s and $\psi = 90°$ of heading .

in an international aerospace engineering competition called called IREC that is held every year in the United States. The objective of this competition is to build, test and fly experimental sounding rockets to achieve as close as possible 10000 ft carrying 10 lb of payload and recover it, thus accuracy is an important aspect.

Two simulators with different formulations are implemented using C++ language and Matlab in order to perform flight simulations. First, a 2 degree of freedom simulator is considered for flight performance analysis and to derive requirements for propulsion and structural subsystems. A computational framework in C++ is developed in order to design the fins of the rocket and ensure its stability during all ascent flight. Finally, a high-fidelity 6DOF simulator is proposed and tested in order to perform Monte Carlo simulations.

The results have shown that the aerodynamic damping coefficients are important to predict flight dynamics of the rocket, but the main performance parameters such apogee and maximum velocity are not hugely influenced by those coefficients. Also, the Monte Carlo analysis have indicated that the horizontal velocity at apogee is greatly affected by wind and that it is a big issue for deriving requirements for the recovery subsystem. Moreover, aerodynamic coefficient errors are responsible for a significant difference in apogee altitude, but not as much as the propulsion model uncertainties. Finally, one of the major contributions of this work is to establish a computational framework for the design of student sounding rockets regarding flight mechanics simulations and their requirements. Later, the authors intended to include

Tabela 5: Parameters distribution for the sensitivity analysis of the final design with Monte Carlo simulations.

Gaussian Distribution		
Parameter	Mean	Standard deviation
Wind velocity	0 m/s	2.3 m/s
Structural mass	21.9 kg	0.11 kg
Launch elevation angle	83°	0.66°
Rail dynamic friction coefficient	0.5	0.1
Ixx($t = 0$)	0.079 $kg \cdot m^2$	0.008 $kg \cdot m^2$
Iyy($t = 0$)	10.743 $kg \cdot m^2$	1.08 $kg \cdot m^2$
Izz($t = 0$)	10.743 $kg \cdot m^2$	1.08 $kg \cdot m^2$
Ixx($t = t_b$)	0.066 $kg \cdot m^2$	0.007 $kg \cdot m^2$
Iyy($t = t_b$)	8.93 $kg \cdot m^2$	0.89 $kg \cdot m^2$
Izz($t = t_b$)	8.93 $kg \cdot m^2$	0.89 $kg \cdot m^2$
CG($t = 0$)	1.61 m	0.021 m
CG($t = t_b$)	1.5 m	0.021 m
Total impulse	7848 Ns	393 Ns
Uniform Distribution		
Parameter	Min	Max
Wind heading	0 °	360 °
Thrust force	1400 N	2000 N
Aerodynamic error	-0.3	0.3

turbulence and more sophisticated wind models in the 6DOF simulator.

5. ACKNOWLEDGEMENTS

The authors gratefully acknowledge the support for the present research provided by Fundação das Indústrias de São Paulo (Fiesp) and Instituto Tecnológico de Aeronáutica (ITA).

6. REFERENCES

Blakelock, J.H., 1991. *Automatic Control of Aircraft and Missiles*. Wiley-Interscience, 2nd edition.

Mueller, P., 2016. "Experimental Sounding Rocket Association Web Page". `http://www.soundingrocket.org`. URL `http://www.soundingrocket.org`.

Nakka, R., 2015. "Richard Nakka Eexperimental Rocketry Web Page". `http://www.nakka-rocketry.net`. URL `http://www.nakka-rocketry.net`.

Stevens, B.L. and Lewis, F.L., 2003. *Aircraft Control and Simulation*. Wiley-Interscience, 2nd edition.

7. RESPONSIBILITY NOTICE

The authors are the only responsible for the printed material included in this paper.

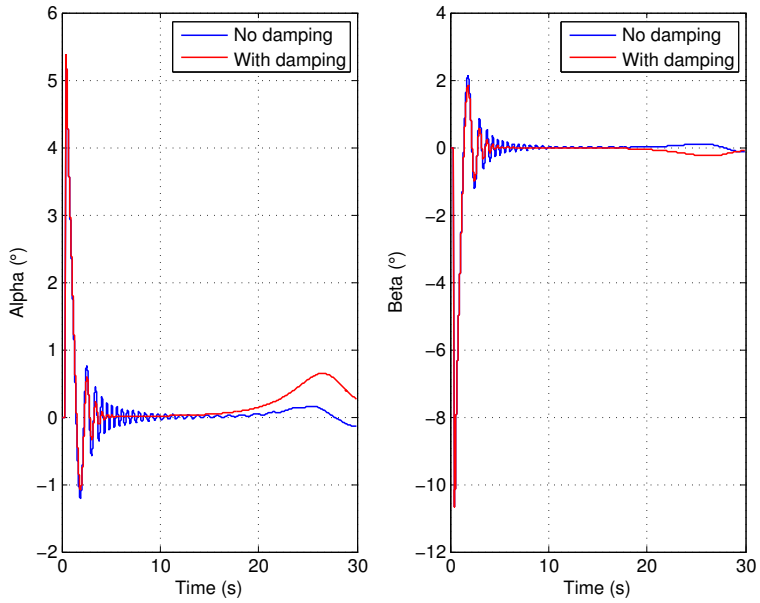

(a) Angle of attack and slip angle curves.

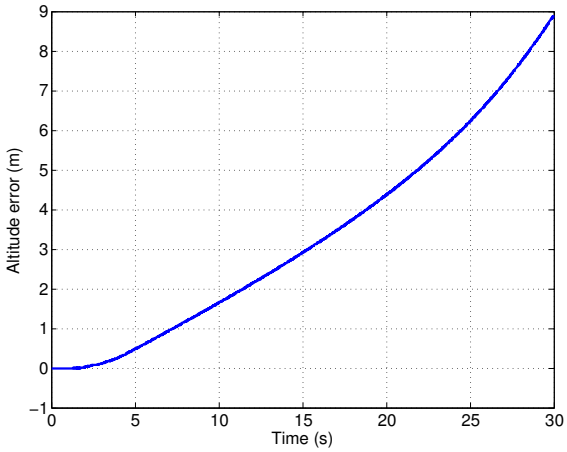

(b) Altitude error.

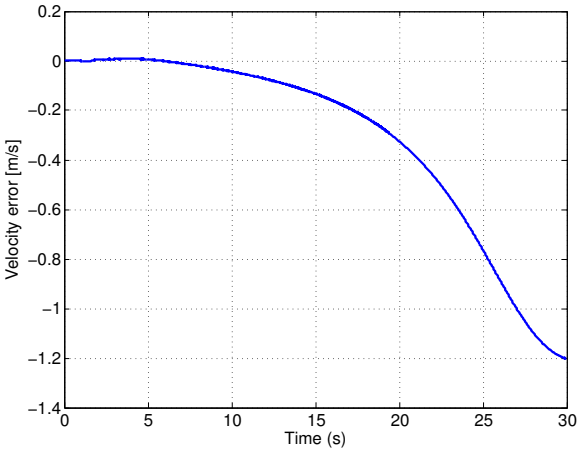

(c) Velocity magnitude error.

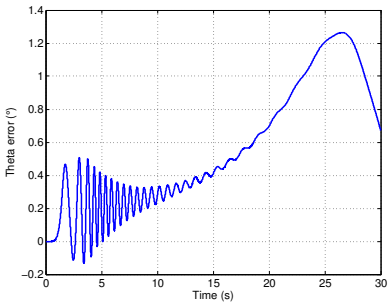

(d) θ error.

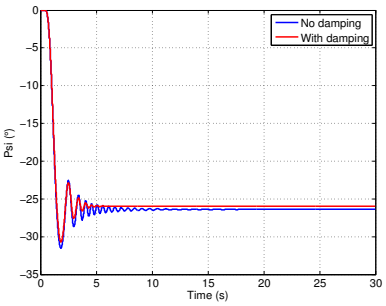

(e) ψ curve.

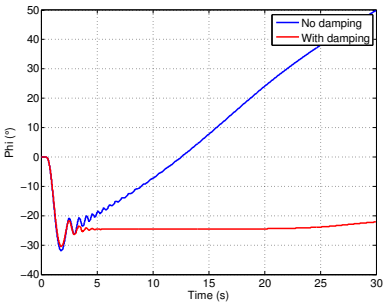

(f) ϕ curve.

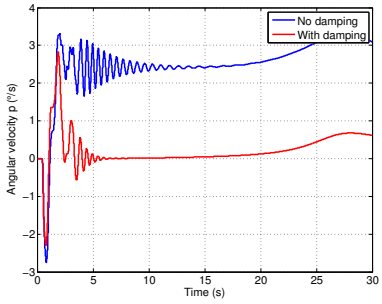

(g) Angular velocity p curve.

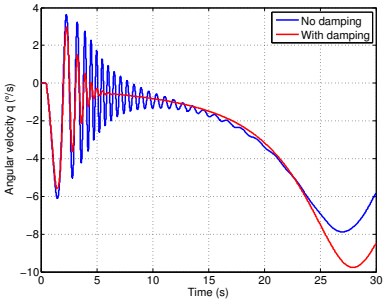

(h) Angular velocity q curve.

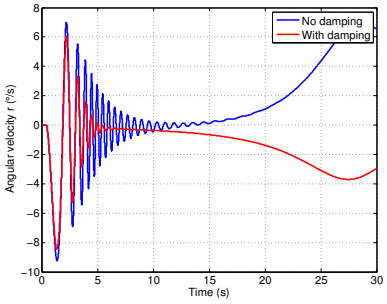

(i) Angular velocity r curve.

Figura 10: Flight simulation with conditions as in Table 3, with and without damping in the aerodynamic model.

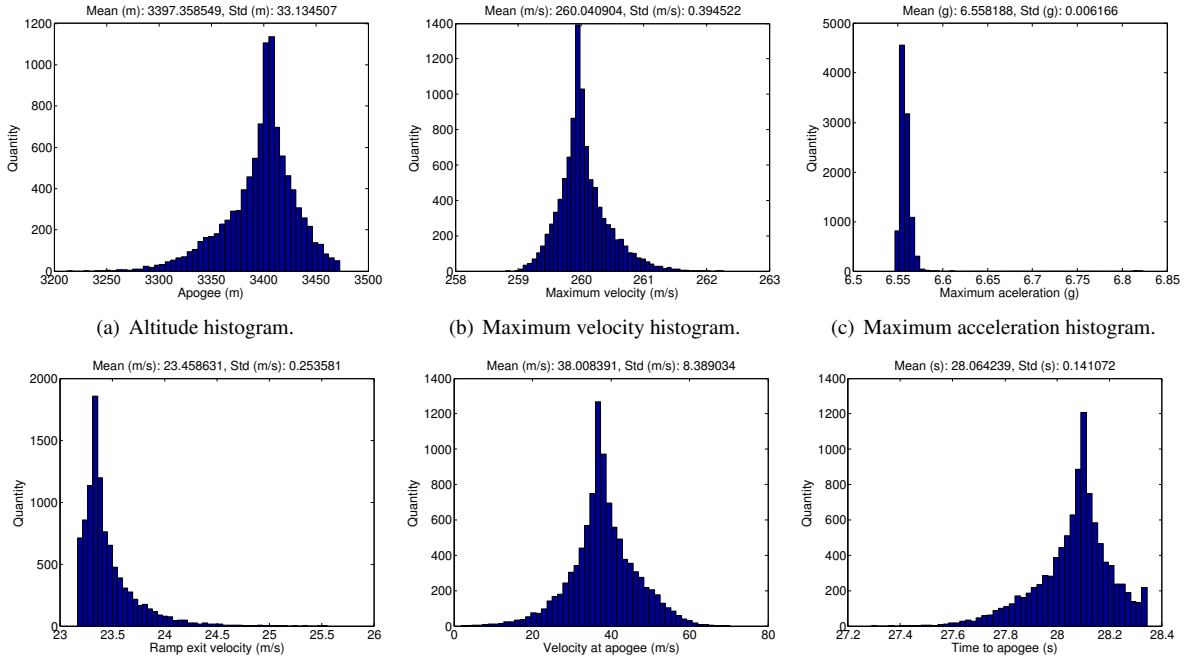

(a) Altitude histogram. (b) Maximum velocity histogram. (c) Maximum acceleration histogram.

(d) Launch rail exit velocity histogram. (e) Velocity at apogee histogram. (f) Time to apogee histogram.

Figura 11: Monte Carlo simulations results for the wind influence.

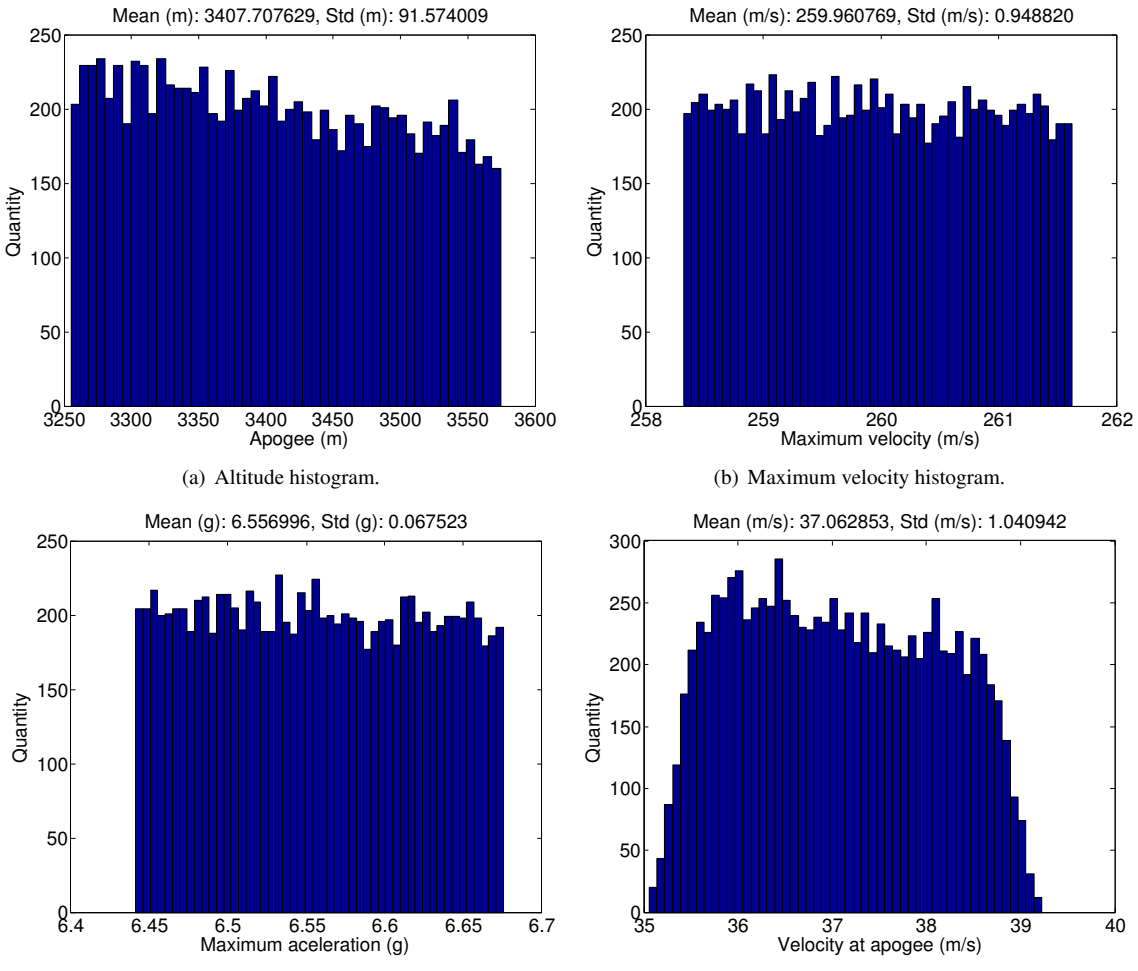

(a) Altitude histogram. (b) Maximum velocity histogram.

(c) Maximum acceleration histogram. (d) Velocity at apogee histogram.

Figura 12: Monte Carlo simulations results for the aerodynamic model uncertainties influence.

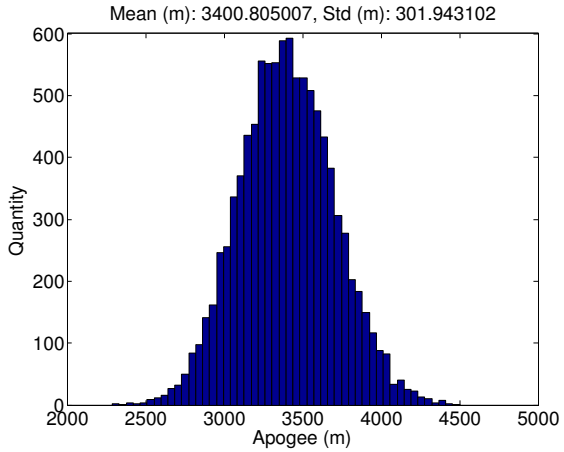

(a) Altitude histogram.

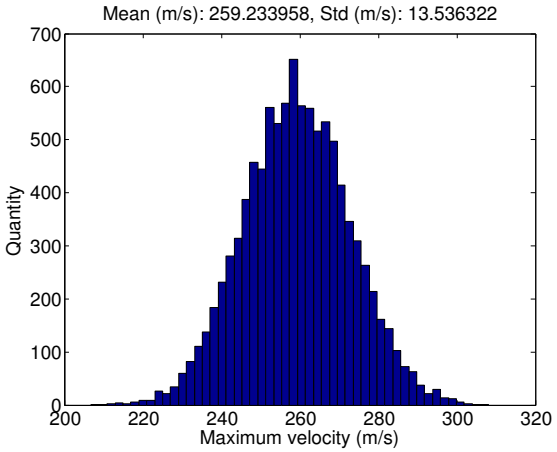

(b) Maximum velocity histogram.

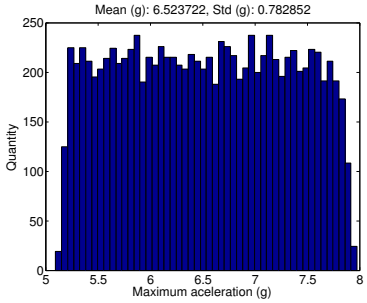

(c) Maximum acceleration histogram.

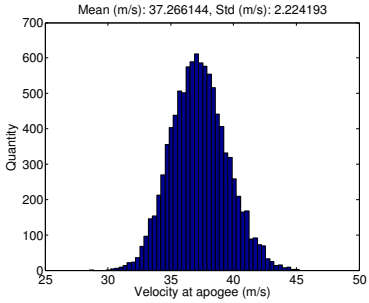

(d) Velocity at apogee histogram.

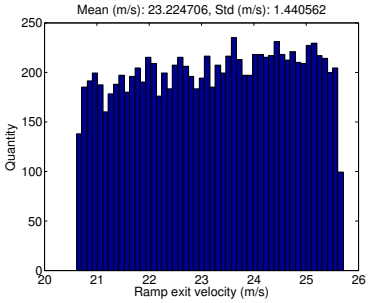

(e) Launch rail exit velocity histogram.

Figura 13: Monte Carlo simulations results for the propulsion model uncertainties influence.

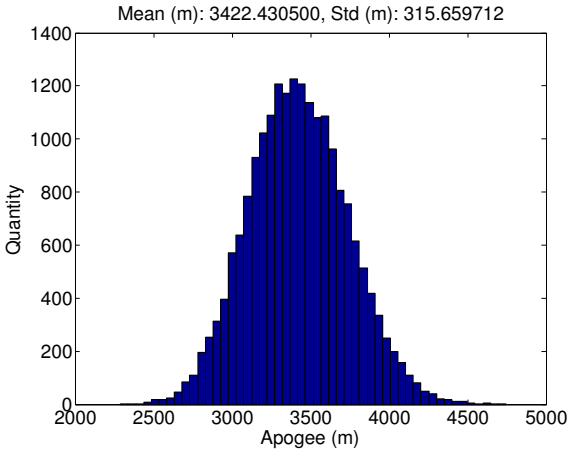

(a) Altitude histogram.

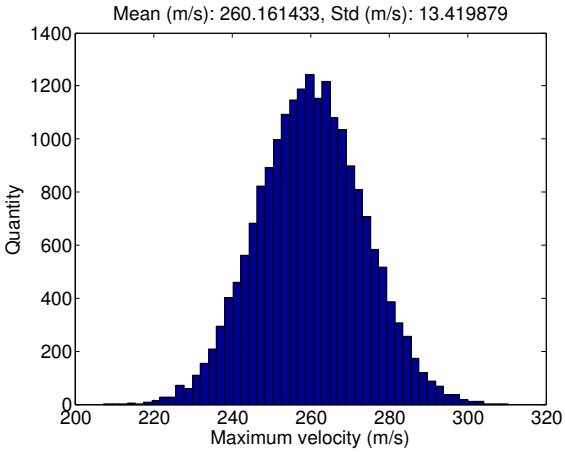

(b) Maximum velocity histogram.

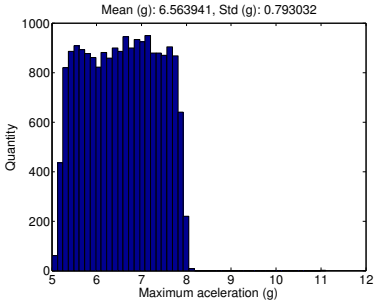

(c) Maximum acceleration histogram.

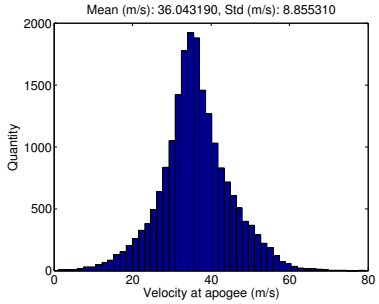

(d) Velocity at apogee histogram.

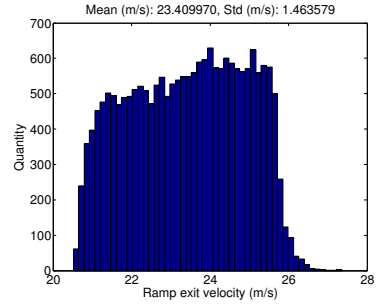

(e) Launch rail exit velocity histogram.

Figura 14: Monte Carlo simulations results varying parameters in propulsion, wind, inertia and aerodynamics models.